Supporting Information

Novel Strategy to Improve the Efficiency Roll-off at High Luminance and Operational Lifetime of Hybrid White OLEDs via Employing an Assistant Layer with Triplet-Triplet Annihilation Up-conversion Characteristics

Yuwen Chen, Dezhi Yang, Xianfeng Qiao, Yanfeng Dai, Qian Sun and Dongge Ma*

Institute of Polymer Optoelectronic Materials and Devices, Guangdong Provincial Key Laboratory of Luminescence from Molecular Aggregates, State Key Laboratory of Luminescent Materials and Devices, South China University of Technology, Guangzhou 510640, People's Republic of China

*Corresponding author:

Dongge Ma, Email: msdgma@scut.edu.cn

Section 1. Supporting Figures:

Section 2. Supplementary Notes:

Section 1. Supporting Figures:

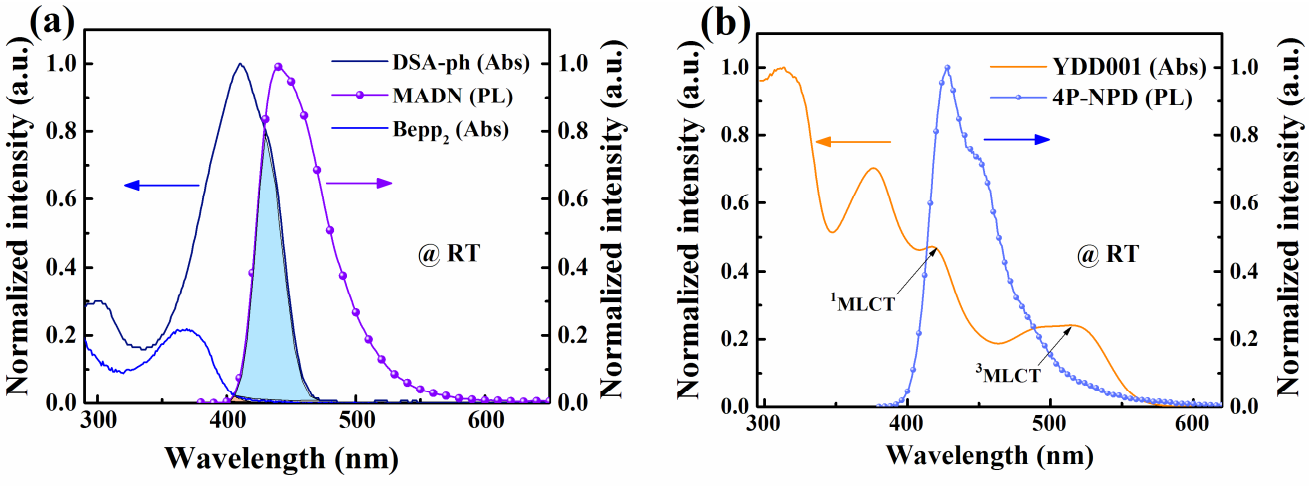

Fig. S1 Photophysical properties of the related materials used in this study. (a) Absorption spectra of DSA-ph and $Bepp_2$, and PL spectrum of MADN films at room temperature (RT). (b) Absorption spectrum of YDD001 as well as PL spectrum of 4P-NPD (1.0×10^{-5} Mol L^{-1}) measured in CH_2Cl_2 at RT.

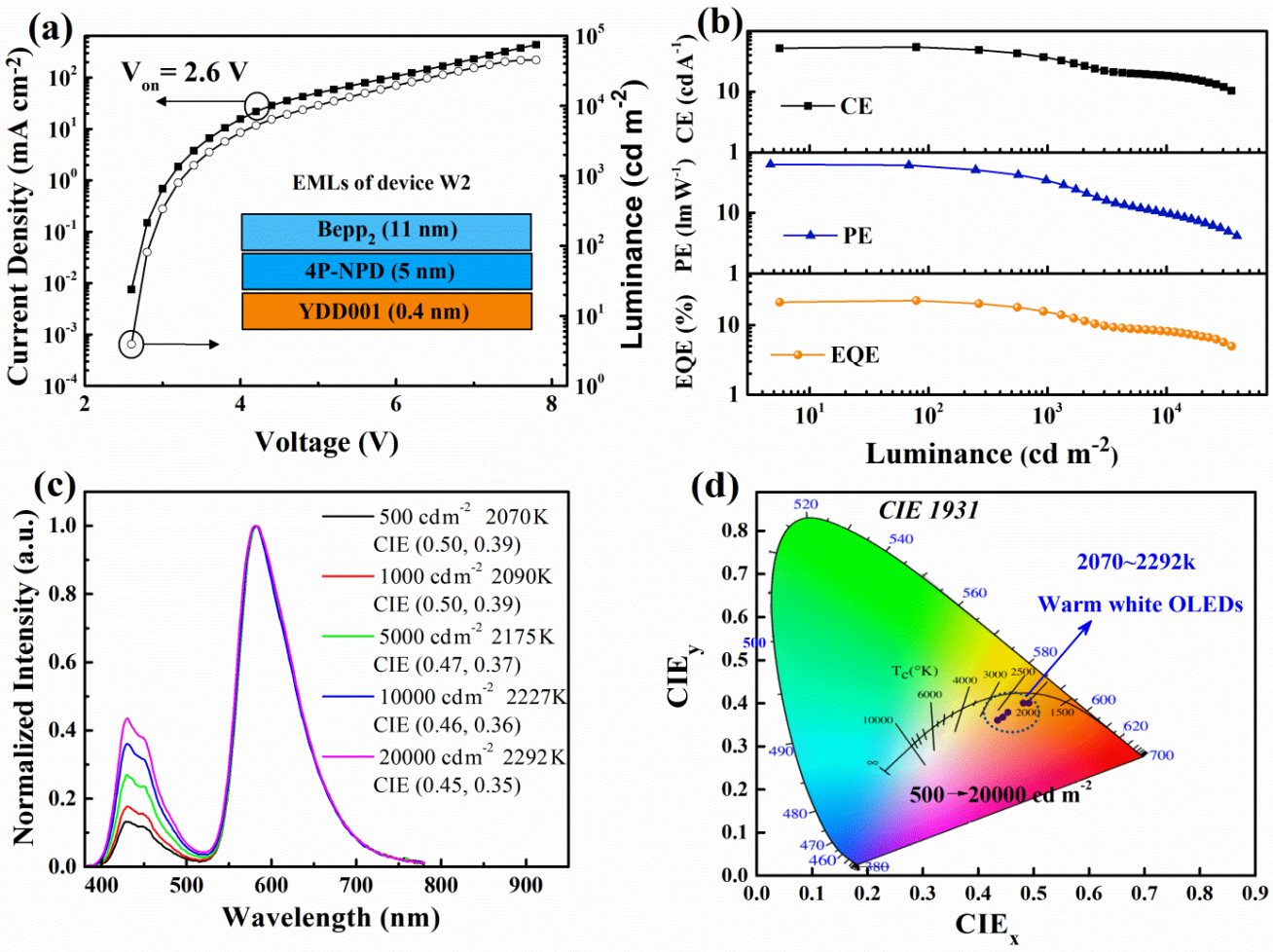

Fig. S2 EL performances of device W2. (a) J–L–V characteristics. The inset shows the structure of EMLs in device W2. (b) Efficiency–luminance curves. (c) Normalized EL spectra at different luminance. The inset shows CCTs and CIE coordinates of device W2 at different luminance. (d) Diagram of CIE of device W2 at different luminance.

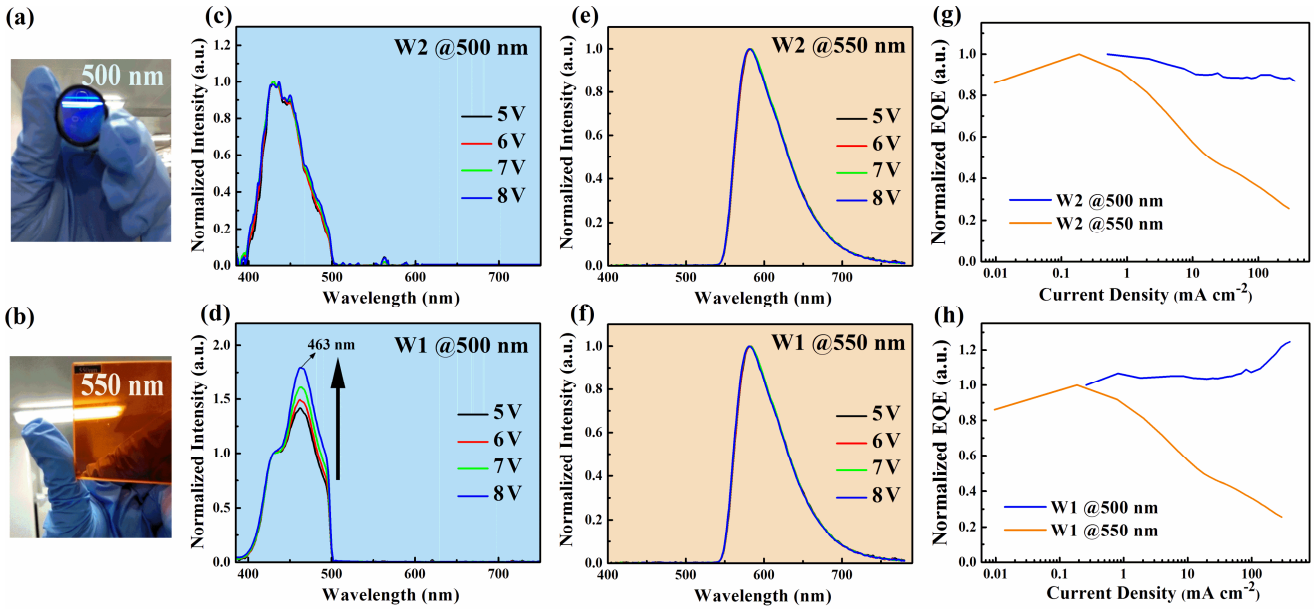

Fig. S3 (a) Image of 500 nm filter for blue emission and (b) image of 550 nm filter for yellow emission in white light devices. Normalized EL spectra of (c) device W2 and (d) device W1 obtained from 500 nm filter at different voltages. Normalized EL spectra of (e) device W2 and (f) device W1 obtained from 500 nm filter at different voltages. Normalized EQE versus current density of (g) device W2 and (h) device W1 obtained from different filters.

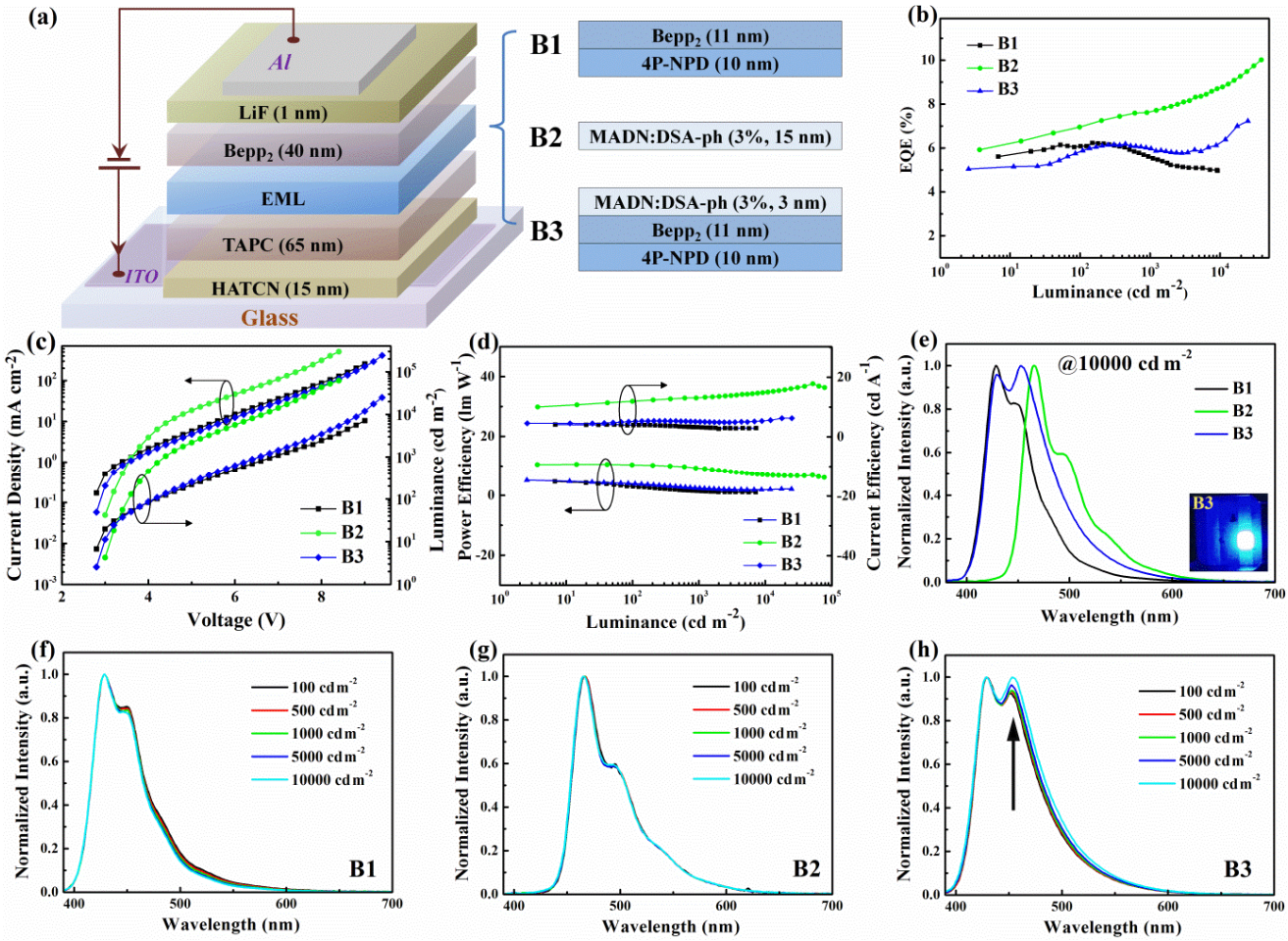

Fig. S4 (a) Schematic layer structures of the fabricated blue OLEDs with three different EML configurations. (b) EQE–L characteristics. (c) J–L–V characteristics. (d) PE–CE–L characteristics. (e) Normalized EL spectra of three blue OLEDs at 10000 cd m^{-2}. The inset shows the EL emission image of device B3 at 10000 cd m^{-2}. Normalized EL spectra of (f) device B1, (g) device B2 and (h) device B3 at different luminance.

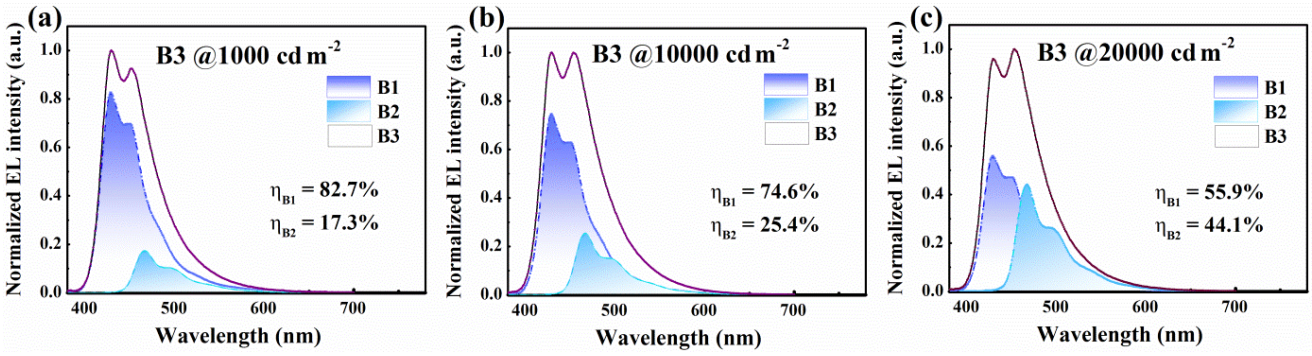

Fig. S5 EL spectra of device B3 at different luminance: (a) at 1000 cd m^{-2}, (b) at 10000 cd m^{-2}, (c) at 20000 cd m^{-2}. The color filled areas refer to the EL spectra of device B1 (4P-NPD/$Bepp_2$) and B2 (MADN:DSA-ph).

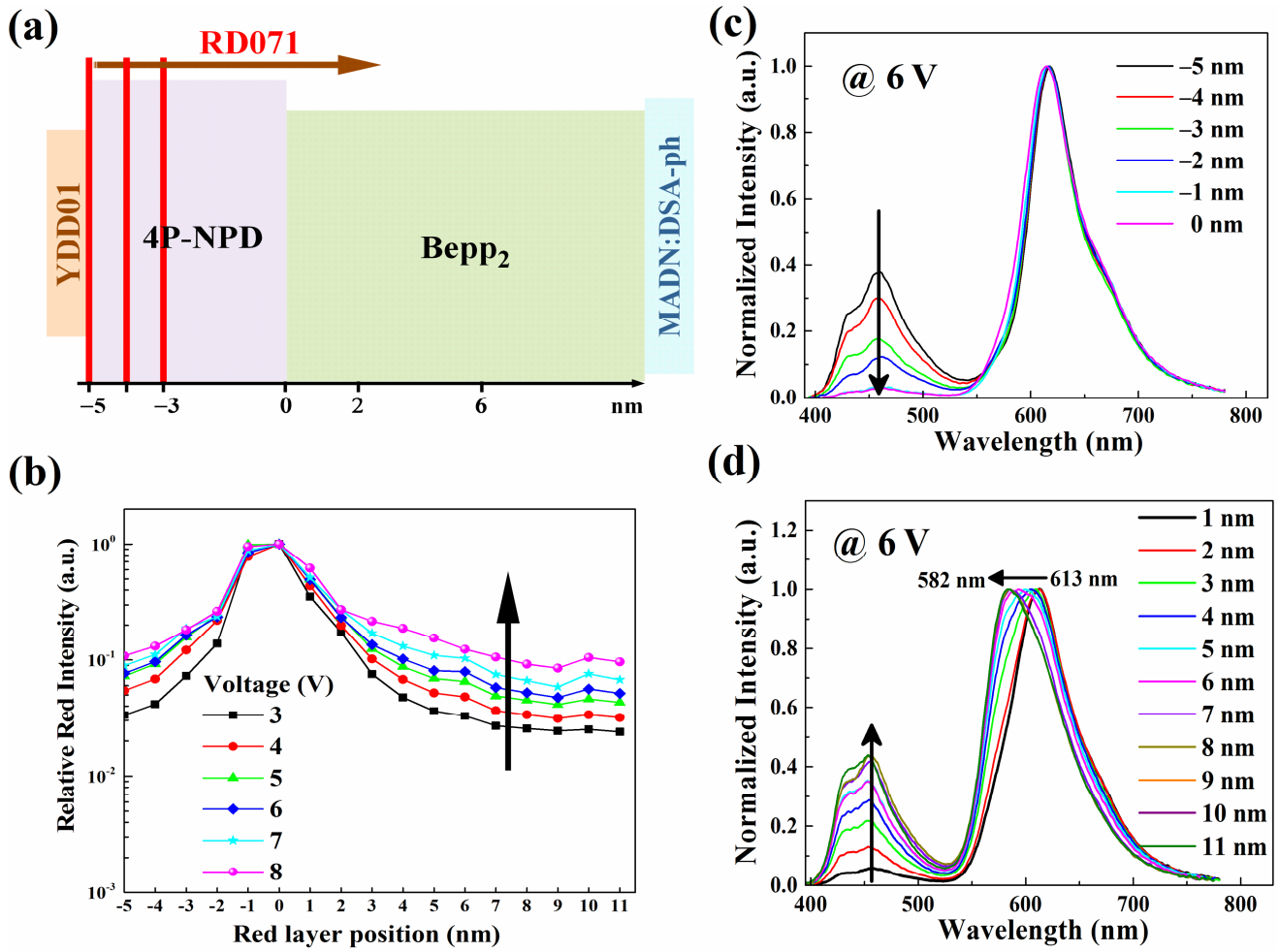

Fig. S6 (a) Schematic diagram of the exploration on exciton distribution in device W1. (b) Relative emission peak intensities of RD071 to 4P-NPD as a function of the RD071 ultrathin layer position in corresponding devices at different driving voltages. The position of the interlayer between 4P-NPD and $Bepp_2$ was recorded as 0 nm. (c) And (d) Normalized emission intensity after inserting the sensing layer located at different positions at 6 V.

Section 2. Supplementary Note:

To study the exciton distribution in device W1, here we used an ultrathin phosphorescent sensor (0.08 nm) to ensure that the inclusion of the sensing strip does not vastly influence the charge transport. Iridium(III)bis[2,4-dimethyl-6-[5-(2-methylpropyl)-2-quinolinyl-N]phenyl-C](2,4-pentanedionato-O2,O4) (RD071) was chosen as the sensing layer because it has very a low triplet energy level of 2.0 eV, and the relative emission intensity can provide some information about the exciton spatial distribution. We explored the exciton density profile in device W1 by using the structure of ITO/HATCN (15 nm)/TAPC (65 nm)/4P-NPD (5 nm)/YDD001 (0.4 nm)/4P-NPD (x nm)/RD071 (0.08 nm)/4P-NPD (5+x nm)/$Bepp_2$ (51 nm)/LiF (1 nm)/Al, and ITO/HATCN (15 nm)/TAPC (65 nm)/4P-NPD (5 nm)/YDD001 (0.4 nm)4P-NPD (5 nm)/$Bepp_2$ (y nm)/RD071 (0.08 nm)/$Bepp_2$ (51−y nm)/LiF (1 nm)/Al, where x varies from −5 to 0 nm, y varies from 1 to 11 nm to change the position of the non-doped yellow phosphor layer (Fig. S6a). As shown in Fig. S6b, the ratio of the red emission peak intensity to the blue intensity (450 nm) as a function of the position of red ultrathin layer at a driving voltage of 3–8 V is given. It can be seen that the red emission (615 nm) is strongest at the position 0 nm that is the interface between 4P-NPD and $Bepp_2$, and remains higher intensity distribution in the range of regions from about −2 to 2 nm. This implies that the exciton recombination zone is mainly concentrated at the interface between 4P-NPD and $Bepp_2$, and extends into 4P-NPD and $Bepp_2$ layers, which further demonstrates the simultaneous emission of 4P-NPB and $Bepp_2$. Furthermore, the normalized EL spectra of these devices are depicted in Fig. S6d, we can see the peak of red emission is shift to yellow emission, which illustrates that the exciton harvesting is different when the red sensors is located at different distances from the interface (between 4P-NPD/$Bepp_2$). This explains that the triplet excitons diffuse as the brightness increases, indirectly.